View metadata, citation and similar papers at core.ac.uk

brought to you by CORE

provided by Online Research Database In Technology

Technical University of Denmark

Deepwind - an innovative wind turbine concept for offshore

Schmidt Paulsen, Uwe; Friis Pedersen, Troels; Aagaard Madsen , Helge; Enevoldsen, Karen; Nielsen, Per Hørlyk; Hattel, Jesper Henri; Zanne, Luca; Battisti, Lorenzo; Brighenti, Allessandra; Lacaze, Marie; Lim, Victor; Wedel-Heinen, Jakob; Berthelsen, Petter A.; Carstensen, Stefan; de Ridder, Erik-Jan; van Bussel, Gerard; Tescione, Giuseppe

Published in:
Proceedings

Publication date:
2011

Document Version
Publisher's PDF, also known as Version of record

Link back to DTU Orbit

Citation (APA):
Schmidt Paulsen, U., Friis Pedersen, T., Aagaard Madsen, H., Enevoldsen, K., Nielsen, P. H., Hattel, J. H., ... Tescione, G. (2011). Deepwind - an innovative wind turbine concept for offshore. In Proceedings European Wind Energy Association (EWEA).

DTU Library
Technical Information Center of Denmark

General rights
Copyright and moral rights for the publications made accessible in the public portal are retained by the authors and/or other copyright owners and it is a condition of accessing publications that users recognise and abide by the legal requirements associated with these rights.

- Users may download and print one copy of any publication from the public portal for the purpose of private study or research.
- You may not further distribute the material or use it for any profit-making activity or commercial gain
- You may freely distribute the URL identifying the publication in the public portal

If you believe that this document breaches copyright please contact us providing details, and we will remove access to the work immediately and investigate your claim.

DEEPWIND-
AN INNOVATIVE WIND TURBINE CONCEPT FOR OFFSHORE

Uwe S. Paulsen[1], Troels F. Pedersen[1], Helge A. Madsen[1], Karen Enevoldsen[1], Per H. Nielsen[1],Jesper Hattel[2], Luca Zanne[3], Lorenzo Battisti[3], Alessandra Brighenti[3], Marie Lacaze[4], Victor Lim[5], Jakob W. Heinen[5], Petter A. Berthelsen[6], Stefan Carstensen[7], Erik-Jan de Ridder[8], Gerard van Bussel[9] , Giuseppe Tescione[9]

Risø DTU Technical University of Denmark, Roskilde, Denmark[1], DTU MEK Technical University of Denmark, Lyngby, Denmark [2],University of Trento,Italy[3], NENUPHAR, Lille, France[4], VESTAS[5], MARINTEK,Trondhjem,Norway[6], DHI,Hørsholm,Denmark[7], MARIN, Nederlands[8], TUDelft,Netherlands[9]

Email:uwpa@risoe.dtu.dk

Abstract:

A European granted project called DeepWind was launched in autumn 2010 under FP7 Future Emerging Technologies. The 4-years project is described and preliminary results from the different work packages are presented. The concept of an offshore floating vertical axis wind turbines (DeepWind) was presented in [1]. The vertical axis wind turbine consists of a Darrieus rotor whose tower is extended below the sea level, in order to act as spar buoy.
This paper informs on new developments within the FP7 project (www.deepwind.eu) of the novel concept and preliminary results from the different work packages of DeepWind are presented.

Keywords: offshore, floating, vertical axis wind turbine, novel concept, aero-elastic code, FP7.

1 Introduction

The project idea emerged from the necessity of technological improvement in offshore wind energy, playing a steadily increasing role and which calls for dedicated technology rather than being based on existing onshore technology transported to sea environment. DeepWind is an attempt to direct offshore wind energy towards, where cost is approximately the same as for onshore MW wind turbines. The DeepWind concept has been described previously on concept technology, challenges and components in [1, 2, and 3].

DeepWind consists of an innovative offshore vertical axis wind turbine (VAWT) concept as shown in Figure 1 . The entire tube system is rotating and the power is generated by a generator placed at the bottom of the tower and fixed with an anchoring system.

The technology combines dedicated solutions and investigations on:

- Feasibility of blade pultrusion manufacture for MW-size VAWT
- Very large slow running direct-drive generators concentric with the turbine shaft, mounted at the bottom of the structure, in deep sea conditions
- Capability of a new control strategy, based on rotational speed control
- Potential of water brakes as a safety system in over-speeding conditions
- Dynamics of a rotating spar-buoy supporting structure
- Anchoring system for a rotating spar
- Fluid interaction at high Reynolds numbers
- Darrieus rotor design.

2 DeepWind S/T methodology

The emphasis is to explore the basics behind the principle, to develop numerical tools, and to verify the concept within the scientific structure as shown in Figure 2.

The project has been divided in nine work packages; six of them reflect the technological challenges within this new field of technology, one the validation of the results, one the integration of the technologies in a 5MW and 20MW design, and one on the dissemination of the results:

1. Aero-elastic code and simulation of performance, dynamics and loads
2. Blade technology and blade design
3. Generator concepts
4. Turbine system controls
5. Mooring, floating and torque absorption systems

6. Exploration of torque, lift and drag on a rotating tube
7. Proof-of-principle experiments
8. Integration of technologies and up-scaling
9. Dissemination and Exploitation

In order to combine the results from the different technologies another dedicated work package deals with project management. An advisory board (L.O.R.C., DNV, Grontmij CarlBro, Sønderjyllands Maskinfabrik, Vatenfall, Vertax Wind LtD) will ensure the connection of the project with the actual needs of the offshore industry.

www.deepwind.eu informs on project background and reveals the current status.

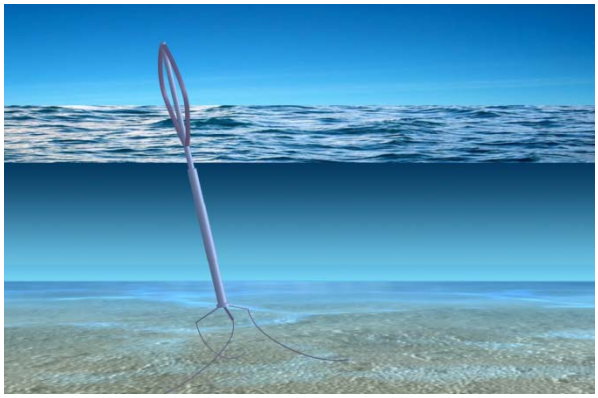

Figure 1: Artistic view of the concept

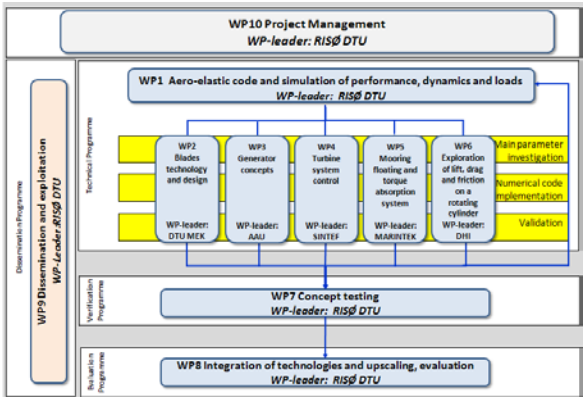

Figure 2: Overall scientific and technical methodology in DeepWind

The progress in development and planning as conducted up to now is presented for work package 1, 2, 5, 6 and 7, for which the content is describes briefly in Figure 3:

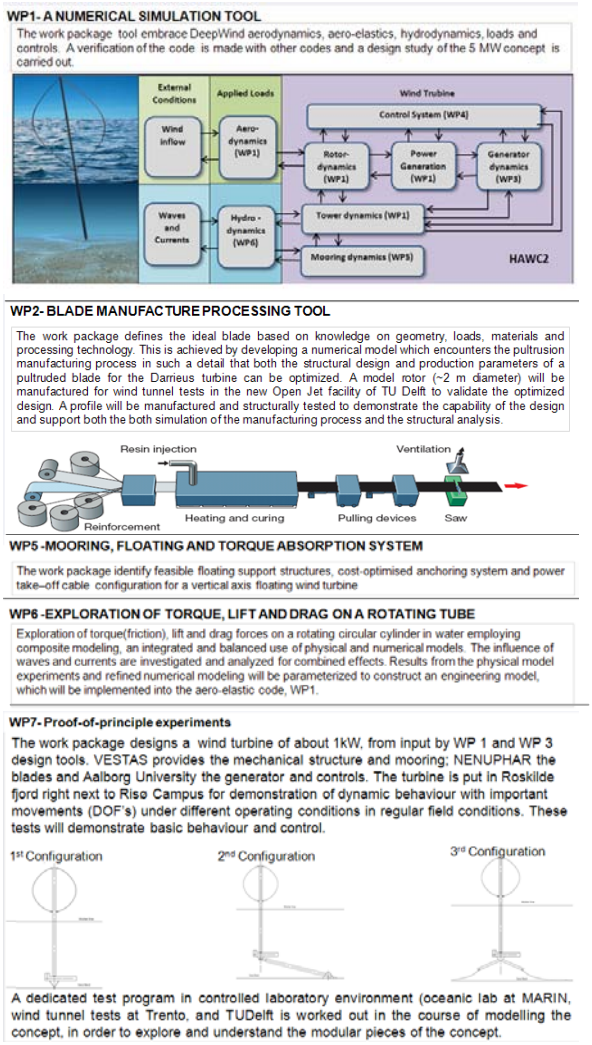

Figure 3: Work package objectives

3 DeepWind WP Progress

3.1 WP1 Numerical simulation tool

3.1.1 HAWC2 simulations

Several configurations are possible in DeepWind. Three of them have been selected to investigate the new concept. The selection is based on the degrees of freedom of the system, defined in Figure 4. The yaw mode consists of the rotation of the rotor itself and it is represents the solid body rotation in all configurations.
Configuration 1: The generator is fixed on the sea-bed and the shaft is extended to the sea bottom. The shaft has two rotational degrees of freedom: it can tilt back and forth and to the sides (pitch and roll).
Configuration 2: The generator is mounted on a torque arm. Compared to the sea-bed configuration the shaft has one more translational

degree of freedom, i.e. it can move up and down (heave).
Configuration 3: Three torque arms are mounted to the generator box. The torque arms are connected to the sea bed by a mooring system. Compared to the previous configuration the shaft has two more translational degrees of freedom (sway and surge).

The simulations with HAWC2 have been carried out on the 1st configuration with rated power of 2 MW. The degrees of freedom of the three configurations are summarized in the table below. Development made in HAWC2 code is described in [2]. The load cases and turbine specs are found in Table 1.

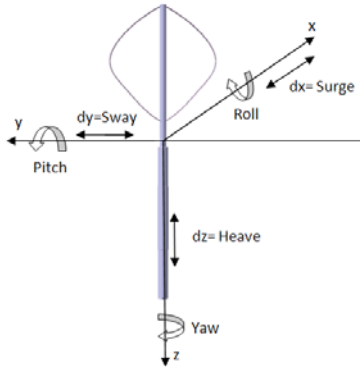

Figure 4: Roll, sway and heave definition

Table 1: DOFs, associated DLCs for the three configurations

	Surge	Sway	Heave	Pitch	Roll
1st Configuration				X	X
2nd Configuration			X	X	X
3rd Configuration	X	X	X	X	X
	Wind		Wave	Current	
1st load case	X		X		
2nd load case	X			X	
3rd load case	X		X	X	

Table 2: DeepWind 2 MW wind turbine key figures

Key figure	Rated number
Power	2 MW
Rotor Diameter	67 m
Rotor Height	75 m
Chord (blades number)	3.2 m (2)
Rotational speed at rated conditions	15.0 rpm
Radius of the rotor tower	2.0 m
Maximum radius of the submerged part	3.5 m
Total tower length (underwater part)	183 m (93m)
Displacement	3000 tons

For DLCs a wind profile with 14m/s strength and power exponent of 0.14 has been selected; the current strength is 1 m/s and considered in a direction perpendicular to the wind; the regular waves have 4 m height amplitude with a 9 seconds wave period.

3.1.2 HAWC2 Results

The resulting trajectory at these conditions is shown in a polar graph for DLC1 in Figure 5 and for DLC2 in Figure 6. In DLC1, the turbine reaches the equilibrium at 5m at the abscissa origin, corresponding to a tilt angle of 3.4°.

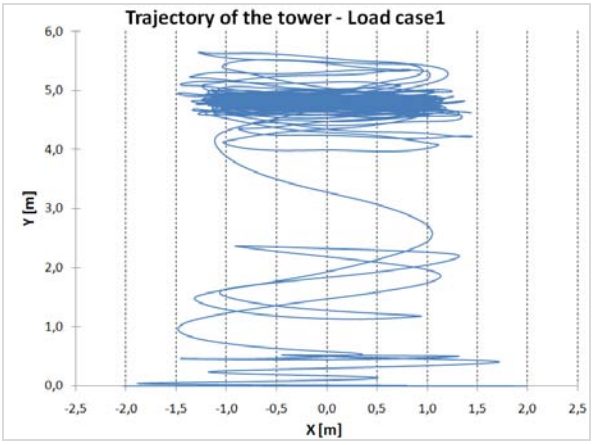

Figure 5: Trajectory of the surface section of the tower in the water surface plane xy

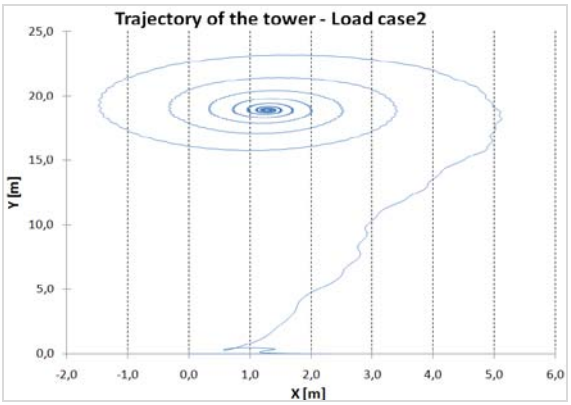

Figure 6: Trajectory of the surface section of the tower in the water surface plane xy

3.1.3 Aerodynamic design and blade profile selection

As a starting point for the aerodynamic performance calculations we took the first draft of the DeepWind demonstrator design of Risø DTU with a 2m rotor diameter and 2m height. The rotor aspect ratio is AR = H/D ≅1.

An annual average wind speed of 5m/s was estimated at the Risø DTU fjord, at a rotor centre which is 2m above the water surface. According to IEC 61400-2 [4] the design wind speed can be derived as 1.4 times the annual average wind speed, i.e. 7m/s.

We performed the simulations with a BEM code, double disk, multiple streamtube, with secondary effects included (dynamic stall, corrections for a finite aspect ratio of the blades, downwind tower wake, flow curvature) at design wind speed.
The calculations were performed with a solidity of 0.2, 0.3 and 0.4 (constant chord) for a 2-bladed and a 3-bladed turbine (H=D≅2m) with $NACA_{0015}$ and $NACA_{0018}$ profiles. The aerodynamic data-base was built with reference data of [5, 6, 7, 8].

We calculated the C_P, $C_{F,X}$, $C_{F,Y}$ as function of the tip speed ratio for the considered rotor configurations. In Figure 7 a comparison between the power coefficient for the two-bladed and three-bladed rotors with the $NACA_{0015}$ profile is presented. The main driver parameter is the solidity, which influences the C_P curve shape and the maximum C_P tip speed ratio. The higher solidities give the best results, due principally to a higher profile Reynolds number at optimum. The maximum C_P is just slightly reduced changing from a two-bladed turbine to a three-bladed one due to the smaller chord of the latter.

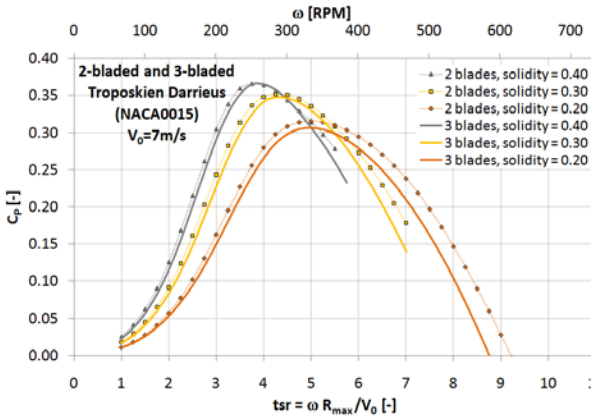

Figure 7: Comparison between the power coefficient C_P versus λ for the $NACA_{0015}$ 2-bladed and 3-bladed Darrieus turbine

For lower solidities the power coefficient curve is broader, with consequently a broader range of rotor speed variability. If we assume smaller rotor inertia due to the lower chord, it would be easier for it to follow the wind speed variability, and it would give a better self-starting capability [9]. The counterpart of working with high rotor speeds are higher centrifugal forces, higher vibrations due to rotor unbalancing, and with sea currents a higher Magnus effect on the submerged part of the tube.
At maximum C_P the streamwise rotor force F_X, the transverse force F_Y and torque were calculated as functions of the azimuthal angle.
In Figure 8 a comparison is presented of the lateral thrust F_Y as function of the streamwise thrust F_X for the two-bladed and the three bladed rotors with the $NACA_{0015}$ airfoil.

There are small differences between a two-bladed and a three-bladed rotor when we look at the average values. But looking at the forces variations, these are about 5-10 times larger for the two-bladed rotors. In the transverse axis the thrust oscillations are much bigger than the average value. It's remarkable that these variations are higher than the streamwise ones in all of the cases.

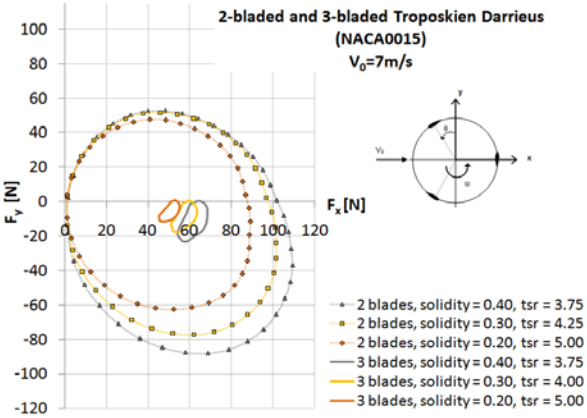

Figure 8: Loads comparison between a 2 and 3-bladed $NACA_{0015}$ Darrieus turbine at maximum Cp

The aerodynamic torque calculations show oscillations that are much higher for the two-bladed rotor compared to the three-bladed rotor. Therefore the latter seems preferable to improve the fatigue life of the mechanical components and to ensure a good electrical power quality. If the experimental rotor is controlled with variable speed control and designed for proper drive train stiffness, damping and rotor inertia calibration, the torque ripple at the generator could be reduced at acceptable levels.

For a constant chord for a 2- and 3-bladed rotor due to mould cost, it would be preferably in the range of 0.095m to 0.107m. This leads to a rotor solidity of 0.22 (B = 2) and 0.33 (B = 3) for the smaller chord and a solidity of 0.25 (B = 2) and 0.37 (B = 3) for the larger chord.

Main results for the different rotor configurations are summarized in Table 3 and in Table 4.

Table 3: Rotor geometry configurations

Rotor Config.	Solidity	Blades Number	Chord [m]	Airfoil
A	0.22	2	0.095	$NACA_{0015\text{-}0018}$
B	0.25	2	0.107	$NACA_{0015\text{-}0018}$
C	0.33	3	0.095	$NACA_{0015\text{-}0018}$
D	0.37	3	0.107	$NACA_{0015\text{-}0018}$

Table 4: Rotor configurations with a $NACA_{0015}$ profile at optimum design conditions

Rotor Config.	λ_{design} (ω [rpm])	$C_{P,design}$ (C_{FX},C_{FY})	Re_{design} min-max $*10^{-5}$
A	4.75 (318)	0.327 (0.671-0.096)	1.71-2.59
B	4.50 (301)	0.338 (0.695-0.110)	1.80-2.78
C	4.25 (284)	0.356 (0.792-0.139)	1.49-2.36
D	4.00 (267)	0.364 (0.809-0.157)	1.55-2.52

Although in the simulations the symmetric $NACA_{0015}$ and $NACA_{0018}$ airfoils have been used, a new airfoil is on the study. It is an asymmetric airfoil designed for VAWT applications, named DU06-W-200. Previous wind tunnel measurements, simulations and operational data on a similar machine have produced promising results [8]. With respect to the $NACA_{0018}$ the new airfoil has an added 2% of thickness and a 0.8% of camber which bring the following advantages:

- an increase in structural strength without a decrease in performance;
- a higher Cl_{max} for positive AoA and a wider drag bucket;
- an improved self-starting property and higher power output at low λ due to the slight camber;
- a deep stall at higher AoA with smaller lift coefficient drop;
- the absence of the laminar separation bubble characterizing the NACA airfoil, which entails a significant noise reduction;
- an increase of the turbine performance at the operating tip speed ratio (for the tested VAWT) of 8% in clean condition and twice as much in dirty condition.

Comparison with the $NACA_{0018}$ can be seen in Figure 9 where airfoil geometry and aerodynamic data are reported.

Simulations of the DeepWind turbine in different configurations are being performed in order to explore the effect of the new airfoil and optimize the design.

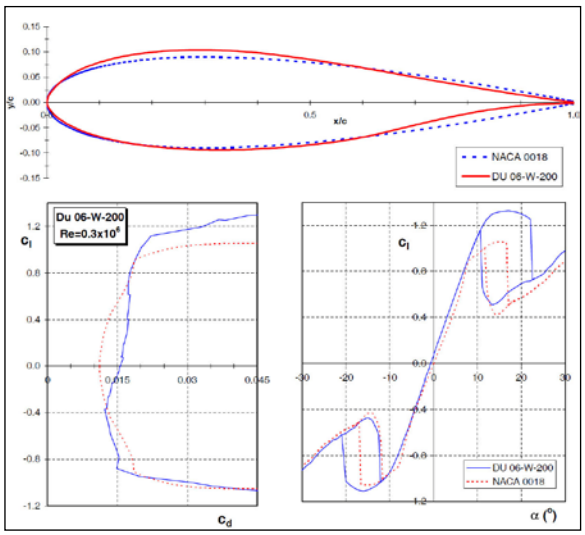

Figure 9: Comparison DU06-W-200/$NACA_{0018}$

3.2 WP2 Blade manufacture processing tool

The work in WP 2 has been concentrated on the blades for the demonstrator turbine.
The demonstrator is the possibility for the group to test blade concepts for the large scale turbine. These efforts are mainly aimed towards the structural design as the aerodynamics are developed using other methods. The main purpose of the design is to provide a functional blade for the demonstrator. The areas where the demonstrator blade can provide information for the general project is in the manufacturing of the blade. The structural design are tailored for composite materials and suited for manufacturing by the pultrusion technology. The technology does not allow for changes in thickness along the length of the blade and moderate thickness changes across the blade are also favored.

Due to the large start-up cost for the pultrusion process the blade is going to be made with conventional production process but effort will be made to simulate the properties of the pultrusion technology. NENUPHAR has developed an innovative blade manufacturing process that optimizes mechanical (dynamic) behavior with a low weight and high stiffness structure. A blade of 7.8 meters has been successfully manufactured.

This manufacturing process is used in DeepWind for exploration of pultrusion technology and can be easily scaled-up for large-size blades. The technology is illustrated in Figure 10.

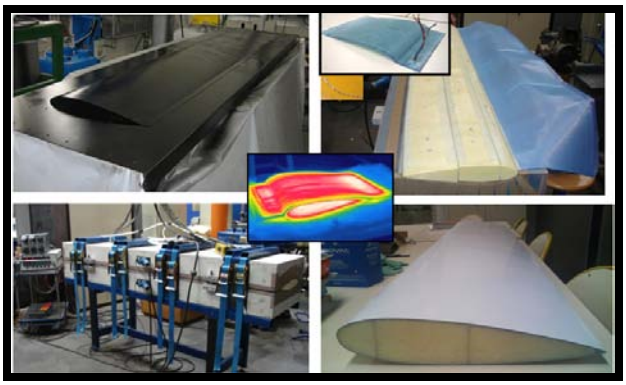

Figure 10: Nenuphar blade technology for pultrusion process study

3.3 WP5 Design of floating support structure and mooring system

The DeepWind concept differs from traditional spar-type concepts known from offshore oil and gas installations due to the rotation of the structure. A very large torque has to be absorbed by the mooring lines at the bottom of the structure. This can be achieved by using rigid arms to connect the tower to the mooring lines and applying sufficient horizontal component of the pretension in the lines in order to absorb this torque.

A recently developed optimization tool, WINDOPT[1] [10,11], will be used to select a cost optimized mooring system and spar type floating support structure. This program utilizes efficient design tools for analysis of mooring system forces and vessel motions, and combines this with a gradient method for solution of non-linear optimization problems with arbitrary constraints.

The optimization in this context is the same as minimizing the material cost while satisfying functional and safety related design requirements. The spar buoy is modelled as composed of a set of cylindrical sections with different mass-, buoyancy- and cost properties. It is assumed that a representative initial cost figure is available, and that it can be scaled in proportion with material mass. The mooring lines are composed of one or more line segments, where the material mass is given as a function of line segment diameter and length.

Design requirements that should be considered are:

- Natural periods in heave and pitch/roll should be larger than the dominating wave periods
- Sufficient vertical stability
- Sufficient roll and pitch stability. Maximum heel angle within an upper limit.
- Maximum acceleration at critical components (e.g. the generator) within an upper limit.
- Sufficient horizontal component of pretension force for minimum yaw stiffness.
- Maximum line tension sufficiently below line breaking strength
- Fatigue life longer than service life

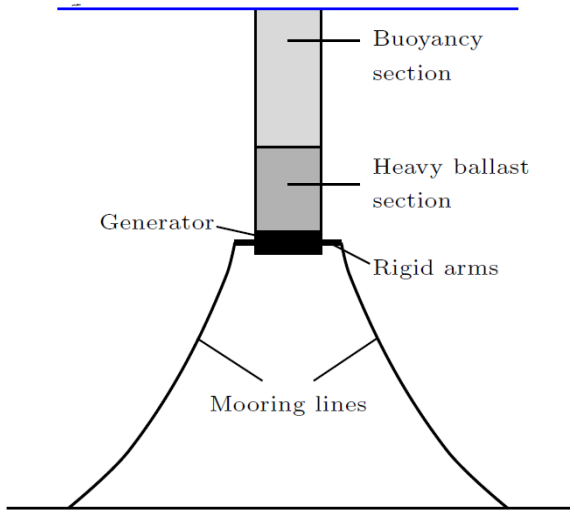

Figure 11: Subsea configuration for cost optimisation analysis

These requirements can be satisfied by manipulating design variables such as spar buoy section lengths and diameters, and mooring line segment lengths and diameters.

3.4 WP6 Exploration of torque, lift, drag on a rotating tube

The flow around the submerged rotating shaft may be broken down into two classic topics within hydrodynamics: (1) Flow around a circular cylinder in current and waves; and (2) Circular cylinder with circulation.

The flow around a circular cylinder in current and waves exert a resultant in-line force (drag) and cross-flow force (lift) on the cylinder. Cylinder diameter, surface roughness and inclination etc. influence the resultant force as well as current speed and amplitude of the wave motion. Generally, the effect of cylinder diameter, D, current speed, U, and the amplitude of the wave motion, a, is expressed in terms of two non-dimensional numbers: the Reynolds number, Re

1 WINDOPT is developed as part of a parallel running research program, NOWITECH – Norwegian Research Centre for Offshore Wind Technology, where the objective is to combine wind technology know-how with offshore and energy industry experience to enhance the development of offshore wind farms.

= DU/υ and the Keulegan-Carpenter number, KC = 2πa/D. Surface roughness is expressed in terms of the relative roughness k_s/D, where k_s is the equivalent sand roughness.

A circular cylinder rotating in water experiences an additional force perpendicular to the motion (lift) known as the Magnus effect. Furthermore, the wall shear stress on the cylinder surface exerts a resultant friction (torque) opposite the cylinder rotation. The rotation may be expressed as the ratio of peripheral speed and the free stream velocity, α = ωR/U.
The hydrodynamic forces are expected to depend to some extend on the specific site and the dimensions of the wind turbine. In non-dimensional terms, however, it is possible to define expected ranges for the governing parameters. Table 5 summarizes the results from an initial analysis of the expected range of governing parameters. In addition to the non-dimensional governing parameters, there are two angles: the tilt angle of the shaft, φ, and the current to wave alignment, θ.

Table 5: Range of expected governing parameters for the hydrodynamic loads

Property		Range	
		Lower limit	Upper limit
Re	= DU/υ	(0 -) $4 \cdot 10^5$	$7 \cdot 10^6$
KC	= 2πa/D	0	15
k_s/D		$0.75 \cdot 10^{-3}$	$3.0 \cdot 10^{-3}$
α	=ωR/U	0	20 (∞)
Tilt angle	φ (°)	0	15
Current to wave alignment	θ (°)	0	90

In work package 6 the hydrodynamics loads on the submerged rotating shaft are being investigated employing composite modelling, an up-to-date combination of physical and numerical models on fluid dynamics (CFD). Laboratory tests help to investigate the underlying physics, while refined models translate the lab results to real-life scale: In the physical model experiments dynamic similarity between physical model experiments and full-scale is only attainable at full-scale due to mutually exclusive scaling laws. The physical model experiments will be scaled using Froude scaling. This means that the Reynolds number is not scaled correctly in the physical model experiments. The consequences of this may are, however, limited because of the surface roughness, especially for a surface roughness close to the upper limit. The CFD model operates at full-scale and is validated against the physical model results and data available in the literature regarding the classic topics. Figure 12 shows the flow close to the submerged rotating shaft in current, waves and rotation. The results are taken from the validation of the CFD model against data available in the literature regarding the classic topics.

The ultimate outcome of the work package will be a hydrodynamic description of the submerged rotating shaft, which will focus on the parameterisation of friction, lift and drag forces for practical engineering use.

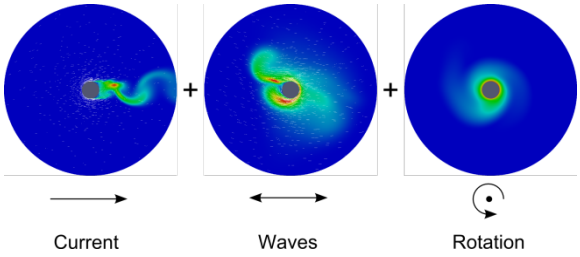

Figure 12: Flow close to the submerged rotating shaft in current, waves and rotation.

3.5 WP7 Testing of concept

In work package 7 design of the 1 kW sized turbine has started along with the specific siting of the turbine in Roskilde fjord at Risø campus.
At the moment Risø DTU and Vestas has started to look closer into 3 different versions of a 1 kW wind turbine mooring spar buoy design: a constant diameter cylinder, 2 cylinders with different diameters joined at the water line; and a cylinder tapered towards the bottom and the top. The most suitable will be equipped with sensors and data monitoring equipment, and the prototype will be designed by Risø DTU, and developed and built by Vestas for the ocean laboratory tests later on in the project.
The plan for first test on a non rotating spar buoy in the fjord is scheduled for this summer and campaigns for the operational unit starting August-September 2011.
The instrumentation design phase is ongoing with proper selection and placement of the sensors, and choice of data acquisition system. Currently the list of measured signals is:

Inside the demonstrator:

- 2x3D accelerometers (top and bottom of tube)
- 1X2D inclinometers
- Electric compass
- DGPS
- Datalogger or Nat. Instr., 100Hz or 400Hz, 1 week battery, on-line wireless transmission

Inside the generator:

- Rotor rpm
- Rotor position
- Power
- Electric compass

On the metmast:

- 3D Sonic
- Cup anemometer
- Current speed
- Current direction
- Wave height
- Wave direction
- Light warning
- Air temperature
- Air pressure
- 2 Video cameras for turbine motion and deflections

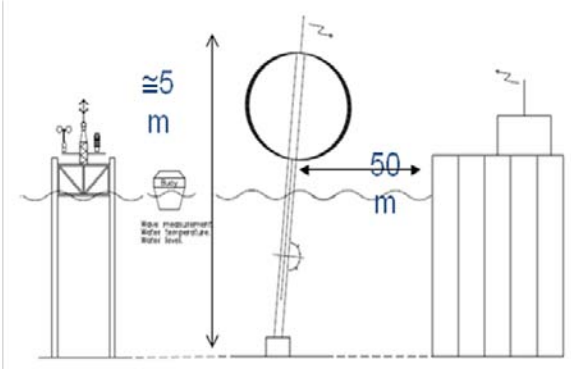

Figure 13: Sketch of experimental demonstrator setup at Risø campus

In 2012 some specific critical conditions for the concept will be picked among the fjord tests and the numerical simulations of DLCs. These conditions will be further investigated in tests conducted under controlled conditions. MARIN's Renewable Energy Team (RENT) will carry out this task in its dedicated Offshore Basin. This basin offers a number of unique possibilities for the modelling of current, waves and wind. Figure 14 shows a cross section of the Offshore Basin.

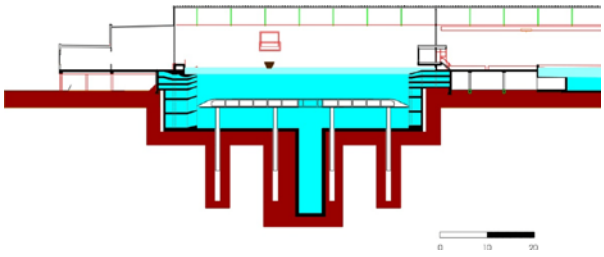

Figure 14: MARIN Offshore Basin

The basin measures 46 m * 36 m and has a movable floor, which is used to adjust the water depth. The maximum water depth measures 10.2 m at model scale. The basin also has a deep pit, with a maximum depth of 30 m.

The model tests are conducted to calibrate/ validate the developed simulation codes within the project and to determine the response of the floating turbine under waves and/or wind conditions, loads on the anchor lines and overall performance for an operational or locked rotor.
Considering the importance of the coupling between the aerodynamic and hydrodynamic behaviour of floating wind turbines, the modelling and documentation of the wind field in MARIN's Offshore Basin during the model tests is of great importance.
However, normal wind quality in a model basin is not good enough for the modelling of the wind for a wind turbine: the local wind generation by small fans does not result in a wind field with the correct vertical profile and with limited turbulence.
To assist in the DeepWind model testing, MARIN is developing at the moment a high quality local wind field modelling setup. This consist of a square bed of 5*5 wind fans (4m*3m) with guides and stators (straighteners), close to the turbine. By controlling the RPMs of the different rows, the vertical profile of the wind can be controlled. The present setup which is under construction is given in Figure 15.

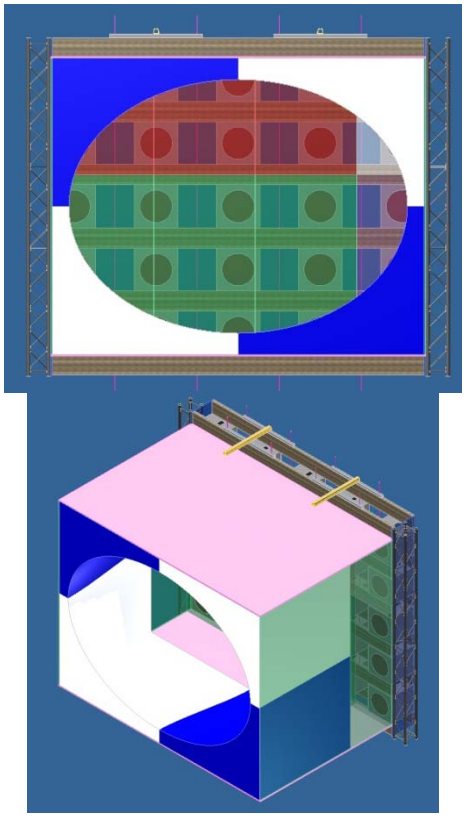

Figure 15: new wind setup for testing floating offshore wind turbines in MARIN's Offshore basin

The above presented windbed is designed with the help of CFD as shown below and will be tested outside the basin to determine and limit turbulence levels.

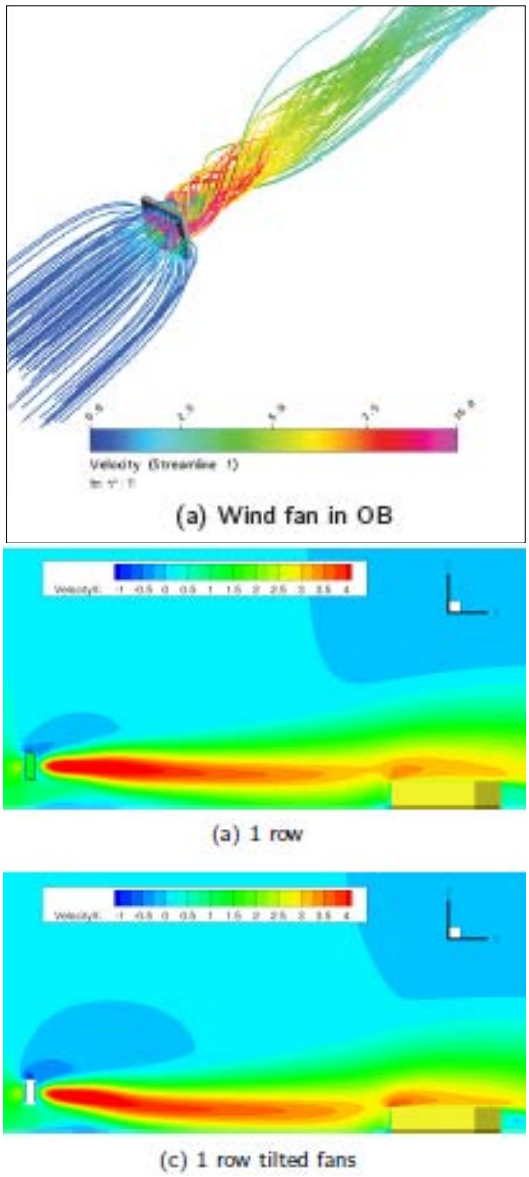

Figure 16 CFD results of the existing wind setup in the model basin

4 Conclusions

In conclusion the preliminary results and experiences from the different work packages show the following:

- Aero-elastic simulation tool performs as planned (WP1)
- A feasible blade manufacturing process is identified to facilitate the pultrusion technology (WP2)
- A feasible cost optimisation tool is ready to be implemented along with a specific design (WP5)
- The test layout for fluid interaction tests ready (WP6)
- The first iteration loop in a 1kW demonstrator design has been started (WP7)
- The design of a engineering based wind array system for tank tests has been started (WP7)

References

1. Vita L, Paulsen US, Pedersen TF, Madsen HA, Rasmussen F A Novel floating offshore wind turbine concept, *EWEC 2009* Vita L, Paulsen US, Pedersen TF, Madsen HA, Rasmussen F A Novel Floating Offshore Wind Turbine Concept: new developments ,- *EWEC 2010* Vita L, Zahle, F., Paulsen US, Pedersen TF, Madsen HA, Rasmussen F A novel concept for floating offshore wind turbines: Recent developments in the concept and investigation on fluid interaction with the rotating foundation, *OMAE2010-20357* International Electrotechnical Commission. Wind turbine. Part 2: Design requirements for small wind turbines. IEC 61400-2:2006-3 (E). 2nd Edition. Geneva: International Electrotechnical Commission.Sheldahl RE, Klimas PC. Aerodynamic characteristics of 7 symmetrical airfoil sections through 180-degree angle of attack for use in aerodynamics analysis of vertical axis wind turbine. Sandia National Laboratories, Albuquerque, New Mexico, SAND80-2114, 1980Timmer WA. Two-dimensional low-Reynolds number wind tunnel results for airfoil NACA 0018. Wind Engineering, Vol. 32, N. 6, pp. 525-537, 2008.Jacobs EN, Sherman A. Airfoil section characteristics as affected by variations of the Reynolds number. NACA Report 586, 1937.
8. Claessens,M.C. Design and Testing of Airfoils for Application in Small Vertical Axis Wind Turbines. The Delft University of Technology, 200
9. Kirke BK. Evaluation of self-starting vertical axis wind turbines for stand-alone applications. PhD Thesis dissertations. Griffith University, Australia, 1998.
10. Fylling I, Berthelsen PA. WINDOPT – An optimization tool for floating supports structures for deep water wind turbines, *OMAE 2011 -49985*.
11. Berthelsen PA, Fylling I. Optimization of floating support structures for deep water wind turbines*, EWEA 2011*.